Monitoring thermal springs to improve land management decision-making, Sierra Nevada, California

Article *in* Environmental and Engineering Geoscience · May 2018

DOI: 10.2113/EEG-1937

5 authors, including:

Jerome V. De Graff
California State University, Fresno

Christopher J. Pluhar
California State University, Fresno

Alan Gallegos
US Forest Service, Pacific Southwest Region, Vallejo CA

Bryant William Platt
United States Geological Survey

Monitoring Thermal Springs to Improve Land Management Decision-Making, Sierra Nevada, California

JEROME V. DE GRAFF[1]
CHRISTOPHER J. PLUHAR

Department of Earth & Environmental Sciences, California State University Fresno, 2576 East San Ramon Avenue, Mail Stop ST-24, Fresno, CA 93740

ALAN J. GALLEGOS
KELLEN TAKENAKA

U.S. Department of Agriculture Forest Service, 1600 Tollhouse Road, Clovis, CA 93611

BRYANT PLATT

Department of Earth & Environmental Sciences, California State University Fresno, 2576 East San Ramon Avenue, Mail Stop ST-24, Fresno, CA 93740

Key Terms: ***Thermal Springs, Land-Use Planning, Site Investigation, Hydrogeology, Sierra Nevada, California***

ABSTRACT

The Sierra National Forest administers Mono Hot Springs and other nearby geothermal features, a concentration of more than a dozen springs, pools, and seeps in the high Sierra Nevada, California. The Native American Mono Tribe traditionally uses Mono Hot Springs for spiritual purposes, while simultaneously the Mono Hot Springs Resort holds a special-use permit for some of the geothermal waters. To support environmental assessments for area management, the Sierra National Forest studied thermal spring chemistry and temperature, evaluating potential use conflicts. An initial multi-year monitoring of 11 representative thermal springs was followed a decade later by another multi-year sampling of the same springs, providing insight into the geothermal character of Mono Hot Springs. Measured water temperatures ranged from 44.5°C to 24.3°C and pH from 8.0 to 7.03, depending upon the thermal spring, higher pH values correlating with lower temperatures. Thermal spring temperatures varied seasonally with higher temperatures in springtime and lower ones in autumn. pH did not exhibit a coherent seasonal variation. Mono Hot Spring temperature decreased and pH increased during the decade-long study period, with even greater longer-term temperature change evidenced at nearby Mono Crossing. Silica and cation geothermometry at Mono Hot Springs suggests that the geothermal waters reached equilibrium with 74–79°C rock at depth at estimated pH of 5 to 6. The spatial distribution of neighboring thermal springs, regional seismicity, and mapped faults suggests that Mono Hot Springs rises along faults running nearly north-south, connecting to Mammoth Mountain and Long Valley, California, 30 km to the north.

[1]Corresponding author email: jdegraff@csufresno.edu

INTRODUCTION

Mono Hot Springs, California, represents a hydrological resource on National Forest System land that needs wise management and also provides insight into the hydrogeologic and tectono-magmatic character of the region. Water resources are a significant component of land management on national forests in the United States, with early objectives including "... securing favorable conditions of waterflows ..." as a primary reason for establishing a national forest (Forest History Society, 2009). This direction reflected the fact that many rivers flow from a source within national forests, especially in the western United States, and foreshadowed the many different water resource uses now common to today's national forests. Present-day water-resource management encompasses streams, reservoirs, natural lakes, and springs and attempts to balance the needs of downstream agriculture and communities, electrical power generation, fisheries and wildlife habitat, and recreational activities. To address how best to manage these sometimes-competing water uses, decision-makers need information developed through studies of specific water resources or management activities that might alter them (De Graff, 1979,

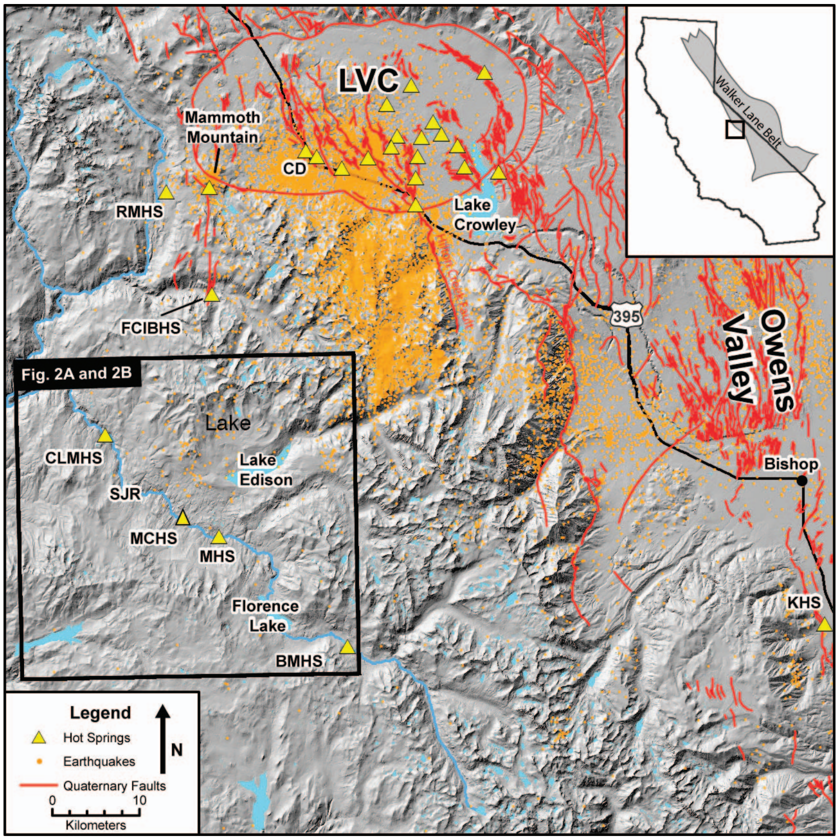

Figure 1. Map showing the region surrounding Mono Hot Springs, including the San Joaquin River South Fork. Figures 2 and 3 are within the outlined area. Among the features shown are Long Valley Caldera (LVC), San Joaquin River (SJR), and Casa Diablo Geothermal Area (CD). Identified thermal springs include Keough Hot Spring (KHS), Red's Meadow Hot Spring (RMHS), Fish Creek/Iva Bell Hot Springs (FCIBHS), Crater Lake Meadow Hot Spring (CLMHS), Mono Crossing Hot Spring (MCHS), Mono Hot Springs (MHS), and Blayney Meadow Hot Spring (BMHS). Data sources: faults USGS and CGS, 2006; seismicity data (August 4, 1980, to August 11, 2016; USGS, 2017); Walker Lane from Dong et al., 2014; thermal spring locations from Berry et al., 1980 and NCEI; hillshade based on USGS 30-m digital elevation (DEM) map.

1982; Jager and Rose, 2003; Berg et al., 2005; and De Graff et al., 2007).

Springs may not contribute greatly to fluvial discharge from a national forest but may constitute significant water resources for wildlife habitat, local potable water, and support of groundwater-dependent ecosystems. Thermal springs are those with a water temperature considerably greater than the local mean annual atmospheric temperature (Neuendorf et al., 2011). A thermal spring is designated as either a "warm" or "hot" spring based on whether its temperature is less than or greater than that of the human body. Thermal springs in national forests are often used for recreation, and a number of these locations are scattered throughout the southern Sierra Nevada. Mono Hot Springs within the Sierra National Forest is a well-known and easily accessible example.

Mono Hot Springs is a concentration of springs, seeps, pools, and concrete structures, clustered adjacent to the South Fork of the San Joaquin River on the boundary of the Ansel Adams Wilderness (Figure 1). The hot springs saw use from pre-Columbian through historic time by Native Americans for spiritual purposes and later development by the federal government and commercial interests in the 1930s and thereafter (Rose, 1994; The Mono Nation, pers. comm., 1999). Today, the site includes a riverside campground and a rustic resort.

Despite their importance to management issues, the character and possible source of Mono Hot Springs' geothermal water have received minimal study (Lockwood et al., 1972; Mariner et al., 1977). The site lies within what is normally considered the "stable" Sierra Nevada batholith but is near Long Valley Caldera and faults of the Walker Lane, as well as a substantial concentration of earthquake epicenters within the Sierra itself (Figure 1; ANSS Comprehensive Earthquake Catalog). In this article, we describe characteristics of Mono Hot Springs, including 1) temperature and pH values and variability identified at individual springs and among the thermal springs in general, 2) decade-long trends in these parameters, 3) the relationship between temperature and pH observed at the springs, and 4) chemical geothermometers applied to several of the thermal springs, providing insight into the geothermal heat source. We also review existing geological and geophysical data in order to speculate on the geothermal system giving rise to this resource.

BACKGROUND

Geologic and Tectonic Setting

The study area lies in the upper San Joaquin River watershed at the eastern-central edge of the Sierra Nevada Microplate, a portion of relatively unfaulted lithosphere between the California Coast Ranges and the Walker Lane (Figure 1; Argus and Gordon, 1991, 2001; Unruh et al., 2003). Despite being in a region of seemingly low deformation rate, one or more factors have or could have contributed to the existence of the Mono Hot Springs geothermal area: 1) tectonic activity of the Walker Lane and Sierra Nevada frontal fault zone located 30 km to the north, northeast, and east along the margin of the Sierra Nevada microplate; 2) volcanic activity of the Long Valley, 30 km to the northeast, and Mammoth Mountain, 30 km to the north (Figure 1); 3) local incipient tectonic activity evident in mapped faults and small earthquakes (Figures 1 and 2A); 4) the Miocene and Pliocene San Joaquin Volcanic Field (Figure 2B); and 5) Sierra Nevada delamination. A review of these follows.

The Sierra Nevada Microplate consists of the Sierra Nevada and the Great Valley physiographic provinces as a single coherent piece of lithosphere (Argus and Gordon, 1991, 2001; Kreemer et al., 2009). The microplate is caught up between motion of the Pacific and North American plates, with most displacement occurring on faults of the San Andreas system and Coast Range faults (Argus and Gordon, 2001) and the remaining 20–25 percent occurring in the Walker Lane and Basin and Range (Dixon et al., 1995, 2000). The Sierra Nevada Microplate moves northwestward relative to stable North America (Argus and Gordon, 1991, 2001; Unruh et al., 2003; and Unruh and Hauksson, 2009), separated from it by the extensional Basin and Range and dextral Walker Lane tectonic provinces (Unruh et al., 2003; Unruh and Hauksson, 2009; Dixon et al., 1995, 2000; and Kreemer et al., 2009). The study area lies within 30 km of the Microplate's eastern edge, where faults mark the Walker Lane, Sierra Nevada frontal fault, and the edge of the Long Valley Caldera (Figure 1).

The Walker Lane hosts numerous distributed faults, hot springs, and geothermal features. North-northwest–oriented dextral faults and north to north-northeast–striking normal faults dominate this belt of dextral to trans-tensional shear (Unruh et al., 2003). The Walker Lane has been active since the Miocene (Surpless et al., 2002; Oldow et al., 2008), with the westernmost Walker Lane, the current edge of the Sierra Nevada microplate, becoming tectonically active between 8 and 3 Ma (e.g., Bacon et al., 1982; Jones et al., 2004; Oldow et al., 2008; and Unruh et al., 2014). Many geothermal features in the Walker Lane derive their heat from tectonically induced magmatic systems, such as the Coso Geothermal Area, which generates ~200 MW of electricity (Monastero, 2002). Others do not exhibit an obvious spatial association with recent volcanic activity (e.g., Keough, Dirty Socks, and Buckeye Hot Springs). Long Valley constitutes one of the most significant concentrations of geothermal features in the Walker Lane (Berry et al., 1980; National Centers for Environmental Information [NCEI]) and includes hot springs such as that at Red's Meadow and Hot Creek, as well as Casa Diablo Geothermal Area, hosting a 29-MW geothermal plant (Mammoth Pacific, 2017).

Today's Long Valley (Figure 1) has been volcanically active since the early Pleistocene (Bailey, 1989) and was the site of one of the most significant Quaternary caldera-forming eruptions in the conterminous United States, producing the Bishop Tuff/Ash (0.772 Ma; Sarna-Wojcicki et al., 2000). Long Valley Caldera experiences earthquake swarms that include probable diking events (Templeton and Dreger, 2006) and surface elevation uplift interpreted to result from magma inflation (Langbein et al., 1993). Long Valley hosts a very active geothermal system (Berry et al., 1980; Hilton, 1996).

Mammoth Mountain, at the boundary between the Sierra Nevada Microplate and Long Valley and 33 km north of the study area (Figure 1), became active during the Pleistocene (0.23 Ma) and continued into the Holocene, most recently erupting ~8 ka (Hildreth et al., 2014; Hildreth and Fierstein, 2016). Earthquake swarms and other seismicity, ground deformation, and magmatic gas release all demonstrate unrest beneath Mammoth Mountain (Sorey et al., 2000; Hill and Prejean, 2005). The magmatic gas release includes CO_2 and mantle helium, emanating from parts of the north, west, and south flanks of Mammoth Mountain, especially to the south near Horseshoe Lake, resulting in tree kills (Sorey et al., 2000; Hill and Prejean, 2005).

In contrast to the tectonically and volcanically active Walker Lane, the Sierra Nevada is relatively quiescent (e.g., Figures 1 and 2A). Earthquakes do occur within the Sierra Nevada Microplate (Figures 1 and 2A), but their magnitudes and abundance (ANSS

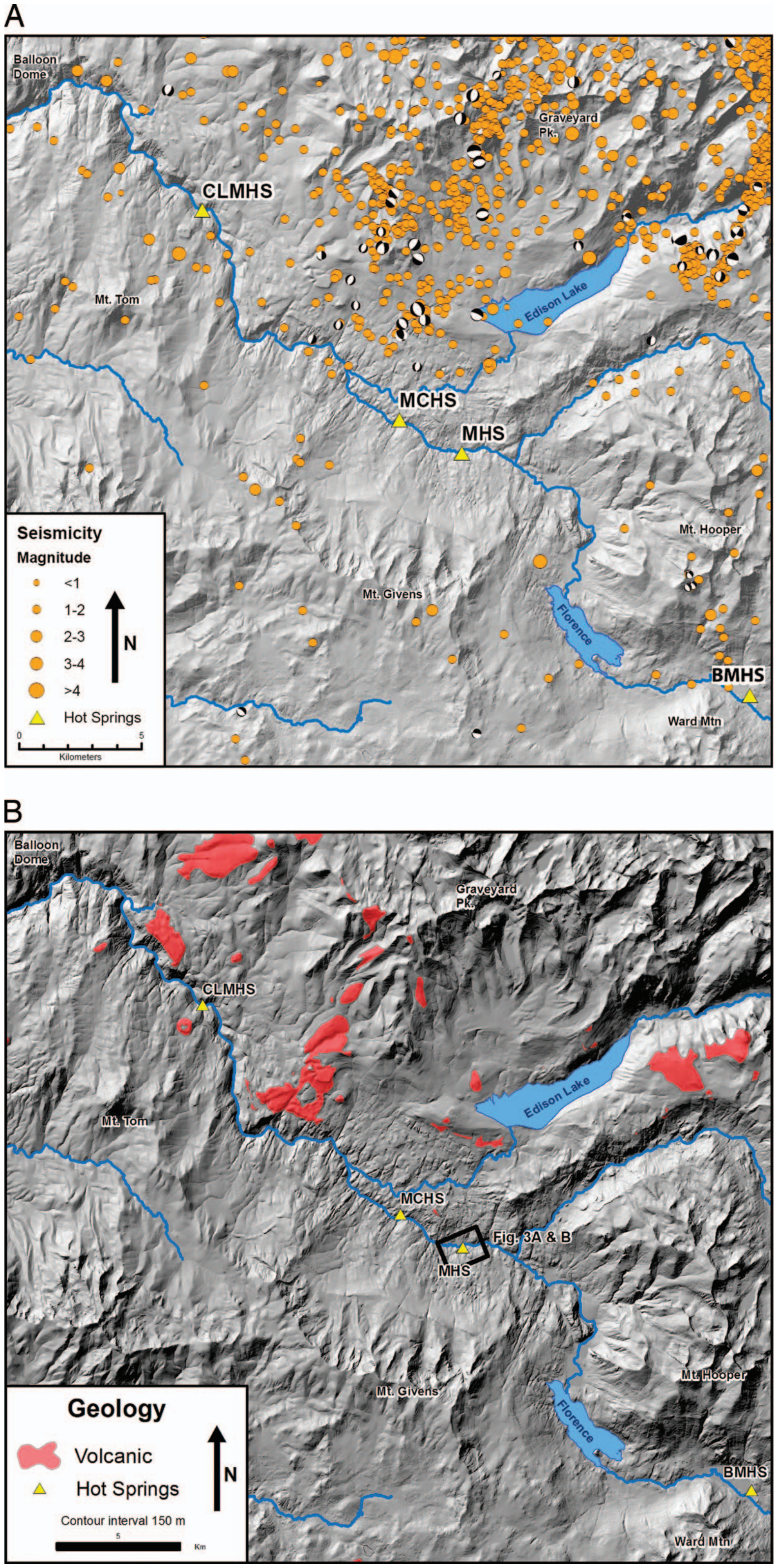

Figure 2. Study area maps, showing Crater Lake Meadow Hot Spring (CLMHS), Mono Crossing Hot Spring (MCHS), Mono Hot Springs (MHS), and Blayney Meadow Hot Spring (BMHS). (A) USGS 30-m DEM hillshade showing earthquake epicenters spanning August 4, 1980., to August 11, 2016 (USGS, 2017), and seismic focal mechanisms for events for which USGS provided them. (B) Topographic map showing remnant volcanic rock of the Miocene and Pliocene San Joaquin Volcanic Field found within the study area (from Bateman, 1965; Bateman et al., 1971; and Lockwood and Lydon, 1975).

Comprehensive Earthquake Catalog) are low compared to the Walker Lane, and Sierran lithosphere experiences little deformation overall (Argus and Gordon, 2001; Kreemer et al., 2009). Very low reduced heat flow measurements (<25 mW/m^2) within most of the Microplate support this idea (Saltus and Lachenbruch, 1991). For the most part, volcanic activity within the Sierra Nevada occurred millions of years ago (e.g., Manley et al., 2000). The study area lies within the Pliocene San Joaquin volcanic field (see Figure 2B), which may have been produced by delamination of an ecologite root and replacement by warm mantle during the Pliocene or late Miocene (Farmer et al., 2002). The volcanic activity near the study area occurred sufficiently long ago that volcanism-associated heat would have already dissipated. Indeed, there is no obvious spatial relationship between Neogene volcanic deposits and thermal springs (Figure 2B). The delamination likely continues to influence regional heat flow in the study area.

However, there are notable exceptions to the current tectonic and volcanic quiescence of the Sierra Nevada. For example, the Cascade Arc's southern terminus, Lassen, lies at the northern end of the Sierra Nevada. In addition, the southern Sierra Nevada currently exhibits significant tectonic and volcanic activity at the Kern Canyon Fault (e.g., Brossy et al., 2012) and nearby hot springs as well as middle and late Quaternary activity in the Golden Trout Volcanic Field (Moore and Sisson, 1985; Manley et al., 2000). Saltus and Lachenbruch (1991) interpreted higher heat flow and seismicity in the southeastern Sierra to represent incipient "calving off" of a segment of the eastern batholith and intrusions at depth, and Unruh and Hauksson (2009) demonstrate seismogenic deformation in the southern Sierra Nevada. In addition, small-magnitude seismicity (ANSS Comprehensive Earthquake Catalog) and small-offset faults (Wakabayashi and Sawyer, 2000, 2001) occur within the Sierra Nevada Microplate at a very low rate (Figures 1 and 2A).

Rocks in the study area are composed of Paleozoic and Mesozoic metamorphic rocks, Jurassic and Cretaceous rocks of the Sierra Nevada batholith, Neogene volcanic rocks, and unconsolidated Quaternary glacial, fluvial, and colluvial sediments and soils (Bateman, 1965; Bateman et al., 1971). Bedrock underlying Mono Hot Springs is the Cretaceous-aged (Tobisch et al., 1995; Frazer et al., 2014) Mount Givens Granodiorite, an extensive pluton within this part of the Sierra Nevada (Bateman et al., 1971). Similarly, the Mount Givens Granodiorite underlies the thermal springs at Mono Crossing and Crater Lake Meadow, both northwest of Mono Hot Springs (Bateman et al., 1971). It may also underlie the Blayney Meadow thermal springs, though the extensive alluvium present and the proximity to other bedrock units makes this determination uncertain (Bateman, 1965). According to Mariner and others (1977), the Blayney Meadow thermal spring present at Muir Trail Ranch issues from granodiorite.

Historical Context

A trans-Sierra trail that passes by Mono Hot Springs facilitated trade between the Mono tribe west of the Sierran crest and tribal groups on the eastern side. The western Mono traditions include both this seasonal trading activity and spiritual use of the springs (The Mono Nation, pers. comm., 1999). The area remained accessible only by foot or horseback until major hydroelectric development stimulated both road and recreational development in the area (Rose, 1994; Sierra Nevada Geotourism, 2017). A road from Huntington Lake across Kaiser Pass was built to facilitate excavation of Ward Tunnel and construction of Florence Lake dam. The tunnel began carrying water diverted from the South Fork of the San Joaquin River in 1925 and then from Florence Lake in 1926. A siphon completed in 1927 still conveys water from the Mono and Bear Creek diversions to the Ward Tunnel, crossing the South Fork San Joaquin just upstream from Mono Hot Springs. In the 1930s, the Civilian Conservation Corps built the High Sierra Guard Station and a bathhouse at Mono Hot Springs. The popularity of the bathhouse resulted in approval of a permit for the Mono Hot Springs Resort.

Opening in 1937, the resort consisted of a general store and a dozen small cabins. Lake Thomas A. Edison was completed in 1954, extending the Kaiser Pass Road beyond the Mono Hot Springs area and facilitating increased recreational access. In the early 1960s, the Forest Service removed bathhouse buildings at the Mono Hot Springs, leaving their concrete foundations in place. At the same time, a spring box and storage tank were built for supplying hot water via a pipeline suspended over the river to a bathhouse at the resort across the river. This bathhouse was rebuilt in the early 1980s.

In the late 1990s, the reissuance of the Mono Hot Springs Resort special-use permit revealed differences among the various stakeholders interested in the management decisions at Mono Hot Springs. The resulting discussions revealed a lack of basic information about the character of the thermal springs. Stakeholders and managers lacked fundamental data, such as the typical temperature and pH of individual springs, as well as spatial and seasonal variability in these factors among the springs. Consequently, the Forest Service initiated a multi-year monitoring program to gather these data. The goal of this monitoring can be described as "phenomena monitoring," the intent of which is to obtain sufficient data to better describe or characterize an event or process (De Graff, 2011). Because national forests cover large areas, land management often requires site-specific studies or monitoring efforts upon which to base decisions (De Graff and Romesburg, 1981; De Graff and Gallegos, 1987; and De Graff et al., 2015). Monitoring was undertaken to improve the understanding of Mono Hot Springs and to provide data with which to underpin future land management decisions affecting these water resources.

Physical Setting

The Mono Hot Springs lie in the southern Sierra Nevada, California (Figure 1). The South Fork of the San Joaquin River flows northwest from its headwaters to its junction with the main stem near Balloon Dome (Figure 2A). In the vicinity of Mono Hot Springs, the glaciated valley of the South Fork is bounded by Mount Givens and the other prominent peaks of Kaiser Ridge on the south and west and the main crest of the Sierra Nevada lying to the east of Mt. Hooper and Graveyard Peak (Figure 2A).

Mono Hot Springs consists of pools, springs, and seeps within an approximately 9-ha area bounded by the South Fork of the San Joaquin River on the north and the Kaiser Pass Road on the east (Figure 3). The main concentration of springs is on the south side of the South Fork of the San Joaquin River across from the Mono Hot Springs Resort (Figure 3). The thermal springs occur within a landscape of granitic bedrock outcrops interspersed with low marshy areas or accumulations of tufa. In a few places, springs flow from either granitic bedrock or tufa deposits. Inflow to pooled water can be detected where gas bubbles rise from the subsurface or by higher temperature zones at pool bottoms. Mariner and others (1977) identified the bubbles in two of the Mono Hot Springs as being predominantly nitrogen and indicative of a lower-temperature thermal system.

The majority of springs rise within pools that are formed in native soil. Some are enclosed within the remnant concrete foundations of historic bath-house structures, where water rises from the open bottom of the foundations. One spring is confined within a concrete box enclosing the spring but leaving the bottom open and permitting a concrete cover to be placed over the top. Water from this spring is piped into a tank supplying the bath house at the Mono Hot Springs Resort via a pipeline across the river. Water outflow from the pools issues through low points, across the top of enclosing concrete structures, or from pipes installed in spring boxes. Thermal spring users have sometimes partially blocked pool water egress in order to raise the water level within a pool.

This study included 11 spring-fed pools scattered across the Mono Hot Springs area (Table 1 and Figure 3). The highest-elevation pools sampled occur at approximately 2,085 m elevation, well above the level of the San Joaquin River (pools 2 and 3; Table 1). Both of these springs form pools within native soil at the base of granodiorite outcrops present on the upslope and downslope sides of Kaiser Pass Road, next to where the road is bridged across the penstock from Lake Thomas A. Edison to the Ward Tunnel (Figure 3). A large accumulation of tufa with extensive warm water seepage occurs on the downslope side of the road adjacent to the west side of the outcrop where pool 3 is located. Roughly downslope from springs 2 and 3, springs 4 and 6 (Table 1) are associated with a large tufa mound along the San Joaquin River's south bank. A concrete bath-house foundation provides a pool for spring 4 at the base of the tufa mound, about 1 m from the river channel, and 4 m above river level (elevation 2,000 m) (Figures 3 and 4A). At 2013 m in elevation, spring 6 issues from the tufa mound apex into a concrete spring box supplying water to a tank for the Mono Hot Springs Resort bath house (Figures 3 and 4B). This spring box is approximately 185 m due south of spring 4 and 17 m higher than the river level. Three spring-fed pools (pools 7, 8, and 9; Table 1) cluster in a flat, open area northeast of the large tufa mound along the San Joaquin River's south bank and 23 m south of the river channel. A concrete bath-house foundation with two deep sections forms the spring 7 pool at about 2,001 m in elevation. Springs 8 (Figures 3 and 4C) and 9 consist of two pools within soil within 3 to 4 m of the concrete structure containing the pool for spring 7. Their elevation and distance from the river channel are essentially the same as those of spring 7. On the bank of the South Fork of the San Joaquin River at an elevation of 1,997 m (within 1 to 2 m of the river, depending on the time of the year), spring 10 supplies a single pool in soil lying 18 m away and almost due north from the cluster formed by springs 7, 8, and 9. Springs 11 and 12 and their respective pools are about 73 m from Kaiser Pass Road. Spring 11 forms a pool adjacent to a large granodiorite outcrop at an elevation of 2,006 m. Spring 12 can be found upslope and to the south of spring 11. Spring 12 supplies one of the larger thermal pools within the top of a small tufa mound at an elevation of about 2,012 m (Figures 3 and 4D). Spring 13 supplies a pool in a small concrete tub similar in appearance to a watering trough and is found at an elevation of 2,023 m at the base of a vertical granodiorite face, just west of the Kaiser Pass Road.

The Mono Hot Springs are not the only thermal springs present along the South Fork of the San

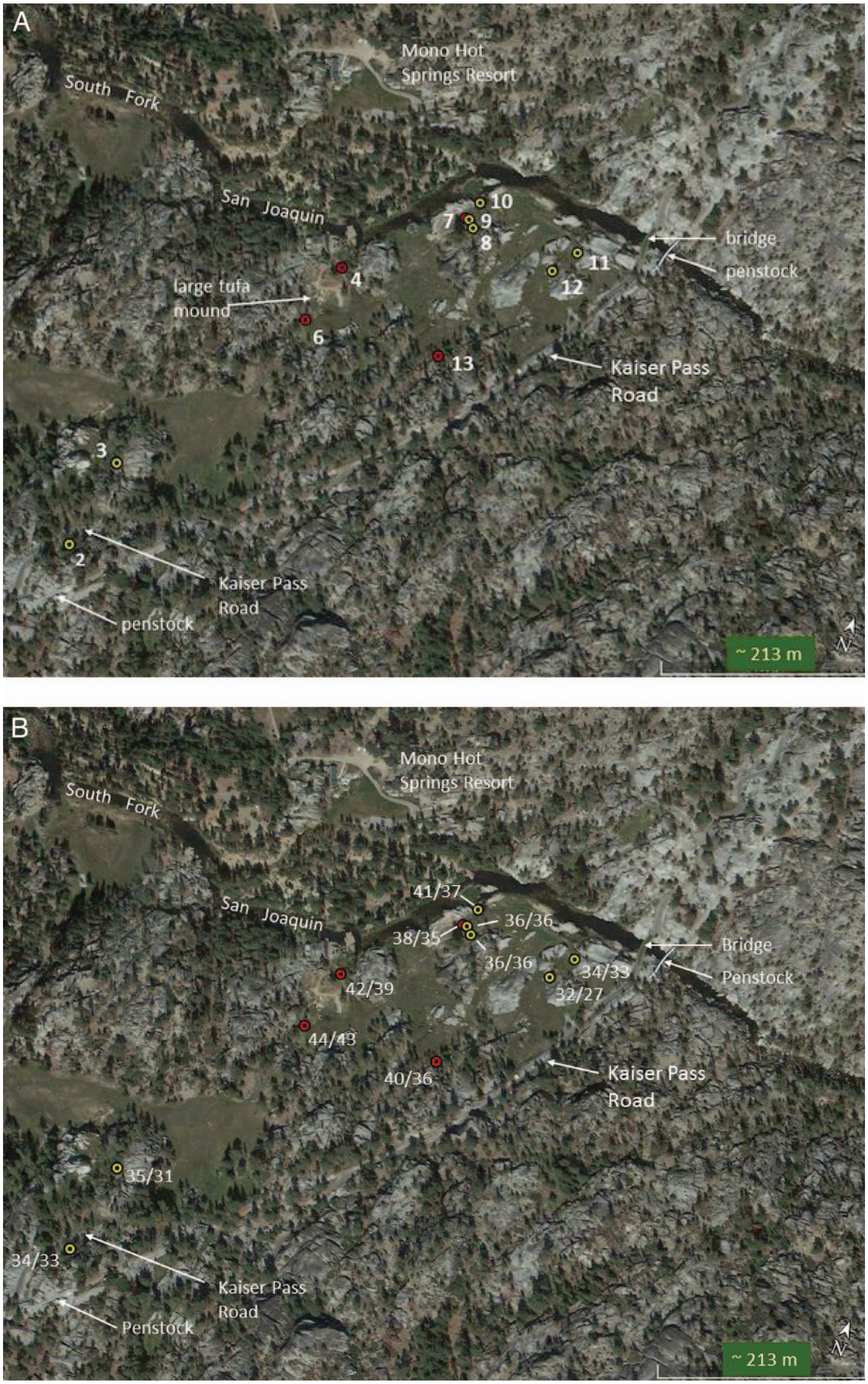

Figure 3. A Google Earth image showing (A) Location of the 11 springs sampled at Mono Hot Springs. The yellow circles indicate the springs formed as a pool in soil, and the red ones are those springs enclosed in concrete structures. The spring numbers correspond to those in Table 1. (B) Average temperature (°C) for the initial monitoring period (Table 2) separated by a slash from the average temperature for the later monitoring period (Table 5).

Table 1. *The 11 pool-forming springs monitored as part of this study at Mono Hot Springs. The spring number, Global Positioning Satellite (GPS) coordinates (WGS-84), description of physical location, and spring description are listed.*

Spring No.	GPS Coordinates	Physical Location	Spring Occurrence
2	N37°19.299′, W119°1.115′	Upslope from Kaiser Pass Forest Road just west of bridge over Edison penstock on small tufa deposit	Natural pool with sandy bottom; gas bubbles observed
3	N37°19.348′, W119°1.108′	Downslope from Kaiser Pass Forest Road and spring 2 on top of large tufa mound	Natural pool with sandy bottom; gas bubbles observed
4	N37°19.501′, W119°1.011′	At the base of large tufa mound just upslope from the South Fork of the San Joaquin River	Double-concrete tub with open bottom, gas bubbles observed
6*	N37°19.464′, W119°1.022′	On the top of the large tufa mound just upslope from the South Fork of the San Joaquin River	Concrete spring box (open bottom) with lockable concrete cover; gas bubbles observed
7	N37°19.556′, W119°0.937′	In the open flat near the South Fork of the San Joaquin River between the large tufa mound and the Bailey bridge crossing	Double-concrete tub with open bottom; gas bubbles observed
8	N37°19.552′, W119°0.932′	In the open flat near the South Fork of the San Joaquin River between the large tufa mound and the Bailey bridge crossing	Small natural pool with sandy bottom; gas bubbles observed
9	N37°19.556′, W119°0.940′	In the open flat near the South Fork of the San Joaquin River between the large tufa mound and the Bailey bridge crossing	Small natural pool with sandy bottom; gas bubbles observed
10	N37°19.568′, W119°0.934′	On the river's edge in the open flat near the South Fork of the San Joaquin River midway between the large tufa mound and the bridge crossing	Small natural pool with sandy bottom augmented by rocks placed on side nearest the river; gas bubbles observed
11	N37°19.561′, W119°0.854′	By a granitic bedrock knob midway between the open flat and the bridge crossing the South Fork of the San Joaquin River	Small natural pool with sandy bottom adjacent to granitic outcrop augmented by rocks placed at the discharge point
12	N37°19.545′, W119°0.867′	At the top of a small tufa mound upslope from spring 11	Natural pool with sandy bottom; gas bubbles observed
13	N37°19.473′, W119°0.923′	Downslope from Kaiser Pass Road and upslope from the bridge crossing the South Fork of the San Joaquin River on small tufa mound	Concrete trough abutting a granitic outcrop; little outflow

*From comparison with information in Mariner et al. (1977) and phone conversation with Dr. Mariner, this spring appears to be the same spring as the one sampled in their report.

Joaquin River (Figure 1). There are other thermal springs in close proximity to the current channel, both upstream and downstream from the Mono Hot Springs. During a geochemical survey, Lockwood and others (1972) found several thermal springs along the South Fork of the San Joaquin River extending 21 km northwestward (downstream) from Mono Hot Springs. However, these springs were described as being cooler than the Mono Hot Springs.

One of these downstream spring locations is about 3 km northwest of Mono Hot Springs near Mono Crossing (Figures 1 and 2). Lockwood and others (1972) described the location as having an extensive area of travertine terraces, similar to features in Yellowstone National Park. A single measurement taken on June 6, 2013, from the only spring visible within that terraced landscape near Mono Crossing yielded a temperature of 18.2°C. The nearly 1.2 ha of travertine terraces and 0.5 ha of tufa deposit imply that several more hot springs previously arose within this area, either in series or simultaneously.

Approximately 21 km northwest (downstream) of Mono Hot Springs, a 35°C thermal spring (http://maps.ngdc.noaa.gov/viewers/hot_springs/) emanates from the north side of the South Fork San Joaquin River Canyon, north of Crater Lake Meadow (Figures 1 and 2). Another concentration of thermal springs is found along the South Fork San Joaquin River about 15 km southeast (upstream) from Mono Hot Springs at Blayney Meadow within the John Muir Wilderness (Figures 1 and 2). The Blayney Meadow thermal springs include a spring issuing from a bedrock fracture at Muir Trail Ranch and a number of spring-fed pools on the opposite (south) side of the river channel. The spring at Muir Trail Ranch is the same one identified by Mariner et al. (1977) as their "Blayney Meadow Hot Spring." The composition of gas in the bubbles rising at Mono Hot Springs and Blayney Hot Spring was found to be 95 and 97 percent nitrogen by volume, respectively (Mariner et al., 1977).

In addition to the thermal springs already mentioned, geothermal features lying to the north of Mono

Figure 4. Representative thermal spring pools from among the 11 monitored between 1999 and 2013 at Mono Hot Springs. (A) Spring 4 is the double-concrete tub at the base of tufa hill near the South Fork of the San Joaquin River. It is representative of several springs rising within the foundations of former bath houses. The snow banks around the spring are typical for mid-winter conditions at Mono Hot Springs. (B) Spring 6 is the spring box at the top of tufa hill. Temperatures measured at this spring were the hottest and varied the least. (C) Spring 8 is a spring pool in soil by the board bridge leading to the deep double-concrete tubs. The temperatures at this spring were found to vary the most during the monitoring periods. (D) Spring 12 is a pool in soil at the top of a small tufa mound upslope from spring 11. Temperatures measured at this spring were the lowest among the 11 springs being monitored.

Hot Springs may also be related. These lie along the surface trace of Quaternary active normal faults striking generally southward from Mammoth Mountain (Figure 1; USGS and CGS, 2006) and include Fish Creek/Iva Bell Hot Spring and the geothermal and magmatic gas release area at Horseshoe Lake just south of Mammoth Mountain. Red's Meadow Hot Spring lies in this general vicinity as well, but off of this linear trend (Figure 1). Mono Hot Springs and Mono Crossings Hot Springs lie along the strike of the Quaternary active faults that run south of Mammoth Mountain, but the mapped faults end long before reaching the study area.

METHODS

Field Temperature and pH Measurements

Field pH and temperature monitoring of the Mono Hot Springs began in October 1999. Subsequently, spring season field pH and temperature monitoring took place once the Kaiser Pass Road was clear of snow, and fall season monitoring occurred after the main tourist season and prior to early snowfall on Kaiser Pass. Between 1999 and 2001, three fall (late September/early October) monitoring events and two spring (late May/early June) monitoring events occurred. Hereafter, this field pH and temperature monitoring will be referred to as the "initial monitoring period."

A decade later another series of monitoring events took place to address ongoing management concerns. This round of monitoring between June 2011 and September 2013 consisted of three spring (early June) monitoring events and three fall (late September/early October) monitoring events. Hereafter, this field pH and temperature monitoring will be referred to as the "later monitoring period."

When initial monitoring began in October 1999, we tested 13 thermal springs distributed across the Mono Hot Springs area. The thermal spring numbers reflect their order during the first field pH and temperature monitoring event and for future reference were named in reference to some identifying site feature. Photos of each thermal spring during this period provided visual reference for future monitoring events. As previously described, these 13 thermal springs consisted of flowing springs and springs rising in pools within soil, springs within concrete bath-house foundations, and one enclosed within a concrete spring box. The two flowing thermal springs proved unreliable for repeated measurement, leaving 11 natural and artificial containment pools fed by thermal springs as the measuring points for the initial 1999–2001 monitoring effort (Table 1). These same 11 pools were evaluated during the later 2011–2013 monitoring period.

Protocols involving both the instrumentation used and field data collection methods were established to ensure the reliability of the monitoring data and to avoid introducing systematic error (Romesburg, 2009). A WTW (Wissenschaftlich-Technische Werkstätten GmbH) Multiline P3 portable meter was used for collecting all temperature and pH measurements during both monitoring periods at Mono Hot Springs, Mono Crossing, and Blayney Meadow (Muir Trail Ranch). This battery-operated meter employs a combined temperature and pH probe. The device was calibrated with standards a day or two prior to each sampling event. We transported the Multiline P3 to and from Mono Hot Springs in the padded plastic carrying case provided by the manufacturer. The senior author or someone under his direct supervision conducted all spring measurements taken with the Multiline P3.

The same protocol was followed during each temperature and pH monitoring event. We collected water in a Teflon plastic cup supplied as part of the equipment for the Multiline P3 device. At a pool, water was dipped by hand with the cup. First, the cup and instrument probe were rinsed with water from the pool. The cup would then be filled by reaching as far below the surface as practicable. In practice, this was usually 40 to 50 cm below the water surface. We strived to collect water closest to where gas bubbles were seen rising to the surface during the initial monitoring event on the assumption the bubbles coincided with the greatest rate of water inflow. During subsequent monitoring visits we attempted to repeat efforts to obtain water at the same point. The temperature and pH probe was placed in the cup of collected water and measurement was initiated per meter instructions. The temperature and pH values were written in a dedicated field notebook along with the spring name, collection date, and time. The order in which the springs were measured was established during the first monitoring event and was generally duplicated in later sampling events. Temperature and pH monitoring typically occurred between late morning and early afternoon.

Geothermometry

Thermal springs gain their heat from deep groundwater circulation to heat sources typically within the upper few kilometers of the Earth's surface (Williams et al., 2008). The impetus of both scientific curiosity and geothermal exploration produced a number of chemical geothermometers for determining the temperature of these deep heat sources (D'Amore and Arnórsson, 1990; Williams et al., 2008). These geothermometers use either silica or various cations found in the emerging spring water to estimate water temperature at depth. These methodologies assume that chemical fluid-rock equilibrium exists in the source aquifer and that the fluid composition remains essentially unmodified as it rises to flow from the thermal spring (D'Amore and Arnórsson, 1990; Williams et al., 2008). Consequently, some thermal spring properties, such as low pH, low thermal spring flow rate, shallow non-thermal groundwater mixing, and localized hydrogeologic conditions (such as rising through salt-rich sediments), can potentially lead to spurious/inaccurate temperature estimates (Mariner et al., 1977; Kolesar and De Graff, 1978; Williams et al., 2008; and Oerter, 2011).

To minimize the likelihood of interference with geothermometer accuracy due to the factors mentioned, three chemical geothermometers were used. Oerter (2011) provides a compilation of silica, cation, and isotope geothermometer formulations with any associated temperature range and source information. The silica (quartz) geothermometer used in this study applies to thermal springs with temperatures ranging from 25 to 250°C (Fournier, 1977). The choice of the Na-K-Ca geothermometer (Fournier and Truesdall, 1973) was partly due to the fact that it is one of the most commonly used cation geothermometers and provides a specific formulation for thermal waters at temperatures of less than 100°C (Williams et al., 2008).

Additionally, both of the foregoing geothermometers were used by Mariner and others (1977), permitting direct temperature comparison between their 1974 Mono Hot Springs #6 sample and our 2013 sampling for the same spring. Williams and others (2008) suggested that a K-Mg geothermometer such as the one developed by Giggenbach (1988) might be more appropriate for non–chloride-rich water, so, we used this geothermometer as well.

In June 2013, we collected water from four of the 11 Mono Hot Springs for geothermometry analysis. The four chosen springs reflect the range of spring temperature and temperature variability and will be fully discussed in the results section. Geothermometry water samples derived from the same location within each spring from which temperature and pH measurements were made. The Teflon cup was rinsed several times in the thermal spring water and emptied on the ground nearby. The cup was then used to fill 1,000-mL amber glass bottles containing nitric acid preservative and 1,000-mL HTPE bottles supplied by the analytical laboratory. All sample bottles were placed on ice in a cooler. Following collection, the samples were transported by vehicle to BSK Laboratories (Fresno, CA) to ensure laboratory analysis within the required hold times.

RESULTS

Temperature and pH of Mono Hot Springs

Temperature

During the initial monitoring period (1999–2001), the 11 thermal springs at Mono Hot Springs yielded instantaneous temperatures ranging between 44.5 and 30.7°C, with variability possibly attributable to spatial factors, physical conditions, or seasonality (Table 2). The average annual temperature for individual

Table 2. *Summary of temperature data. These data include instantaneous temperature measurements, seasonal average temperature within each monitoring period, average temperature for each monitoring period, and range of temperature within each monitoring period. The mean values for the seasonal averages are in bold at the bottom of their respective columns.*

Spring (°C)	#	19-Oct-99	31-May-00	17-Oct-00	5-Jun-01	23-Oct-01		Fall Mean	Spring Mean	Ave. Temp	Range Diff.
Roadside Pool (above Little Eden)	2	33.6	35.1	33.4	34.9	33.3		33	35	34	1.8
Little Eden	3	34.5	36.1	35.4	35.7	34.0		35	36	35	2.1
Double Concrete Tub (@ base of Tufa Hill)	4	41.1	42.4	41.3	42.1	41.4		41	42	42	1.3
Spring Box @ top of Tufa Hill	6	44.5	44.2	44.3	44.1	43.9		44	44	44	0.6
Deep Double Concrete Tubs	7	38.5	38.7	37.6	37.3	36.1		37	38	38	2.6
Spring by Board Bridge (to Deep Dbl tubs)	8	35.4	40.3	32.8	39.1	32.3		34	40	36	8.0
Spring to North of Deep Dbl concrete tubs	9	34.2	39.1	33.4	37.6	34.7		34	38	36	5.7
Parisol Pool (next to river)	10	41.2	41.6	40.6	40.2	40.6		41	41	41	1.4
By the Rock Pool	11	40.5	42.4	41.5	38.3	41.3		41	40	41	4.1
Pool Above "By the Rock"	12	32.4	35.2	30.7	33.0	30.7		31	34	32	4.5
Little Tufa Mound Spring Box	13	39.9	41.5	39.7	41.4	36.4		39	41	40	5.1
								37.3	**39.1**		

Spring (°C)	#	16-Jun-11	14-Oct-11	5-Jun-12	20-Sep-12	7-Jun-13	30-Sep-13	Fall Mean	Spring Mean	Ave. Temp	Range Diff.
Roadside Pool (above Little Eden)	2	33.1	31.9	30.4	33.0	36.2	31.2	32	33	33	5.8
Little Eden	3	33.1	30.4	28.9	31.4	34.8	29.8	31	32	31	5.9
Double Concrete Tub (@ base of Tufa Hill)	4	41.9	40.3	37.7	36.7	42.3	38.0	38	41	39	5.6
Spring Box @ top of Tufa Hill	6	43.2	n/s	n/s	42.5	43.7	40.7	42	43	43	3.0
Deep Double Concrete Tubs	7	37.5	35.1	33.8	35.6	36.6	34.0	35	36	35	3.5
Spring by Board Bridge (to Deep Dbl tubs)	8	38.9	34.3	36.8	33.4	38.8	32.6	33	38	36	6.3
Spring to North of Deep Dbl concrete tubs	9	38.2	35.4	35.8	35.7	38.7	33.9	35	38	36	4.8
Parisol Pool (next to river)	10	n/s	38.0	36.3	36.6	39.2	36.3	37	38	37	2.9
By the Rock Pool	11	38.4	38.1	35.3	36.9	39.1	37.5	38	38	38	3.8
Pool Above "By the Rock"	12	30.9	24.5	26.8	24.3	29.8	26.0	25	29	27	5.5
Little Tufa Mound Spring Box	13	37.5	34.8	n/s	n/s	38.1	35.1	35	38	36	3.0
								34.6	**36.7**		

thermal springs ranged from a high of 44°C at spring 6 to a low of 32°C at spring 12. Results also demonstrate that individual thermal springs exhibited unique temperature variability during the initial monitoring period. At one end of the variability spectrum, temperatures at the spring box on top of the large tufa mound (spring 6) fluctuated only 0.6°C, whereas at the other end of the spectrum the thermal spring by Board Bridge (spring 8) seasonally oscillated across a range of 8.0°C (Table 2). The monitored thermal springs were found to vary during the year, showing temperature maxima in spring and minima in fall.

During the later (2011–2013) monitoring period, the 11 thermal springs at Mono Hot Springs produced instantaneous temperatures ranging from 43.7 to 24.3°C (Table 2). Again, the highest average annual temperature was at spring 6 (43°C) and the lowest was at spring 12 (27°C) (Table 2). In addition, the difference between the greatest and smallest temperatures recorded for individual thermal springs revealed that some springs varied more than others, similar to findings from the initial monitoring period. As before, the least variable thermal spring was spring 6 at the summit of the large tufa mound, with a difference of only 3.0°C. The thermal spring by Board Bridge (spring 8) again exhibited the greatest difference at 6.3°C (Table 2). The seasonal temperature variability again displayed a maxima in spring and minima in fall.

The average annual thermal spring temperatures exhibit no obvious spatial or surface characteristics–related pattern (Figure 3). We considered all of the following factors, and none provided a clear influence on water temperature: location/elevation within the study area, type of spring containment, distance from the river channel, or proximity to other springs with similar temperature characteristics. For example, spring 6, which has the highest average temperature and little seasonal temperature variability, is only 1 m higher in elevation than spring 12, which has the lowest average temperature with the greatest variability in seasonally measured values. The nature of the spring pool and proximity to the San Joaquin River appear to play no role in thermal spring temperature. For example, springs 4 (contained within a bath-house foundation) and 10 (a within-soil pool) are found at nearly the same elevation only tens of meters apart and are the two thermal springs located closest to the river (within 1 to 2 m), yet both thermal springs produced some of the higher average temperatures of the 11 springs monitored. Temperature variability appears to be unrelated to water temperature between thermal springs in close proximity. Both springs 11 and 12 display a similar moderate variability in their temperature measurements over time, but the average annual temperature of spring 11 is among the higher ones measured, while spring 12, located only 25 m away and 6 m higher on the slope, has the lowest average temperature.

Seasonality could influence thermal spring temperatures through mixing with shallow groundwater from snowmelt. The mean thermal spring seasonal (fall and spring) temperatures were computed for the initial monitoring period (Table 2). The mean annual temperature for early fall monitoring (late September to early October) was 37.3°C, while the value for late spring monitoring (late May to early June) was 39.1°C (Table 2). The autumn temperatures at the 11 thermal springs were consistently lower than or equal to those taken during springtime. A similar comparison for the mean thermal spring seasonal (fall and spring) temperatures was computed for the later sampling period (Table 2). The mean annual temperature for early fall monitoring (late September to early October) was 34.6°C, while the value for monitoring done during late spring (late May to early June) was 36.7°C (Table 2). Comparison of these mean seasonal values for the initial and later monitoring periods demonstrates a consistent 2°C difference between mean fall and mean spring temperatures.

In order to test the statistical significance between the mean seasonal thermal spring temperature differences, we applied the Kolmogorov-Smirnov (K-S) test, a non-parametric and distribution-free method applicable to our uncertainty about the nature of the population distribution and suitable for the relatively small number of data points (Cheeney, 1983). An Internet-accessible program for computing the K-S was used to make these calculations using all of the initial monitoring period measurements taken in the fall compared to those taken in the spring (CSBSJU, 2016).

Table 3 displays the results of the K-S test comparing fall and spring temperatures for the initial (1999–2001) and later (2011–2013) monitoring period and the descriptive statistics for their respective fall and spring temperature populations. For the initial (1999–2001) monitoring period, the maximum difference in cumulative fraction or sample K-S statistic is $D = 0.3485$, with a P value of 0.062. For the later (2011–2013) monitoring period, maximum difference in cumulative fraction is $D = 0.3118$, with a P value of 0.082. In both cases, the sample statistic is greater than the critical D statistic (Zaiontz, 2016) for the same P value. So we reject the null hypothesis that the fall and spring temperature values are all drawn from the same population during both initial (1999–2001) and later (2011–2013) monitoring periods. This indicates that a statistical difference exists between the mean fall and spring temperature populations during both the initial (1999–2001) and later (2011–2013) monitoring periods.

Table 3. *The descriptive statistics for seasonal temperature for each monitoring period with their respective Kolmogorov-Smirnov (K-S) statistic values. Also provided are the descriptive statistics comparing temperature and pH data between the two monitoring periods.*

Groups	No.	Mean	Standard Deviation	High	Low	K-S Test Results
Initial monitoring period fall temperatures	33	37.31	4.14	44.5	30.7	D = 0.3485, with P = 0.062
Initial monitoring period spring temperatures	22	39.10	3.20	44.2	33.0	
Later monitoring period fall temperatures	31	34.32	4.30	42.5	24.3	D = 0.3118, with P = 0.082
Later monitoring period spring temperatures	31	35.86	5.02	43.7	20.2	
Initial monitoring period temperatures	55	38.03	3.86	44.5	30.7	D = 0.2903, with P = 0.120
Later monitoring period temperatures	62	35.09	4.70	43.7	20.2	
Initial monitoring period pH values	55	7.35	0.245	7.8	7.0	D = 0.3429, with P = 0.001
Later monitoring period pH values	62	7.52	0.197	8.0	7.15	

Visually, it would seem that the later monitoring period average annual temperatures are nearly all consistently cooler by a few degrees than the average annual temperatures during the initial monitoring period (Figures 3 and 5). To test the statistical significance of this apparent difference, the K-S test was applied to the distribution of all the temperature measurements for the initial (1999–2001) monitoring compared to those of the later (2011–2013) monitoring period (Table 3). The maximum difference in cumulative fraction is D = 0.2903, with a P value of 0.120. We reject the null hypothesis that the initial and later monitoring period temperatures are drawn from the same population because the sample statistic is greater than the critical D statistic (Zaiontz, 2016). From this, we conclude that a statistically significant temperature difference exists between the earlier and later monitoring periods, in addition to the seasonal variation found between spring and fall temperature within each monitoring period.

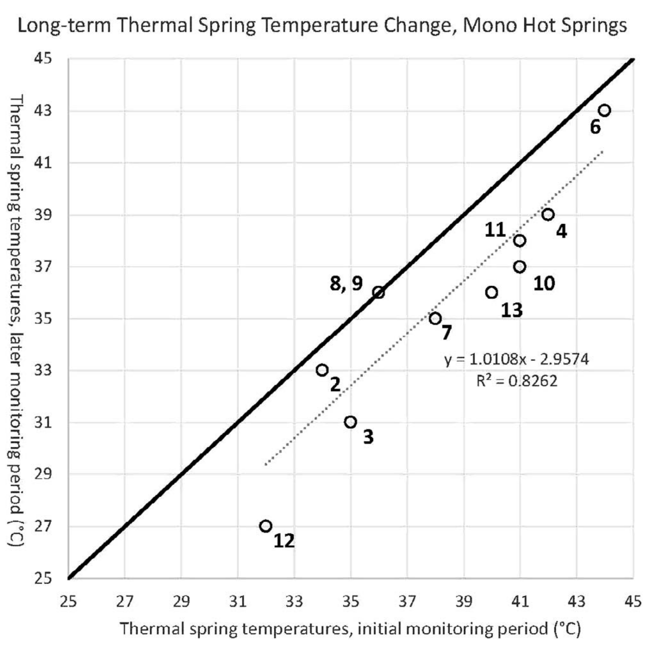

Figure 5. Plot of springs and average annual temperatures for both the initial and later monitoring periods. The actual data show a trend line (dashed) subparallel to the 1:1 line with a temperature offset of about 3°C, indicating that the initial monitoring period temperatures were generally warmer than the later monitoring period temperatures. The formula on the graph is the regression defining the data points relative to the trend line.

pH

The initial monitoring period revealed pH values ranging from 7.0 to 7.8, whereas the later monitoring period obtained similar pH values of between 7.15 and 8.0 (Table 4). The mean pH for the 11 thermal springs during the initial monitoring period was 7.35 and for the later monitoring period was 7.52. Figure 6 shows an observable relationship of higher pH values associated with lower temperatures in both monitoring periods. While this linear relationship is not identical for both monitoring periods, they are similar. The coefficient of determination (R^2) for the line fitted to the data accounting for 78 percent of the variability present during the initial monitoring period and 62 percent of the variability for the later monitoring period.

Given the statistically significant temperature differences between initial and later monitoring periods, a similar assessment of pH was warranted (Table 3). The K-S test yielded D = 0.3429 at P = 0.001. The sample D value is greater than the critical D statistic (Zaiontz, 2016) for the same P value, meaning we reject the null hypothesis that the initial and later monitoring period pH values are drawn from the same population. Therefore, a statistically significant increase in pH between the initial and later monitoring periods exists concomitant with a decrease in temperature. In contrast to the seasonal temperature variation and long-

Table 4. *Summary of pH data. These data include instantaneous pH measurements, seasonal average pH within each monitoring period, average pH for each monitoring period, and range of pH within each monitoring period.*

Spring	#	19-Oct-99	31-May-00	17-Oct-00	5-Jun-01	23-Oct-01		Fall Mean	Spring Mean	Ave. pH	Range Diff.
Roadside Pool (above Little Eden)	2	7.36	7.36	7.62	7.29	7.35		7.4	7.3	7.4	**0.33**
Little Eden	3	7.62	7.62	7.47	7.59	7.69		7.6	7.6	7.6	**0.15**
Double Concrete Tub (@ base of Tufa Hill)	4	7.11	7.11	6.99	7.07	7.21		7.1	7.1	7.1	**0.22**
Spring Box @ top of Tufa Hill	6	7.06	7.06	6.98	7.03	7.03		7.0	7.0	7.0	**0.03**
Deep Double Concrete Tubs	7	7.28	7.28	7.22	7.37	7.51		7.3	7.3	7.3	**0.29**
Spring by Board Bridge (to Deep Dbl tubs)	8	7.72	7.72	7.73	7.55	7.83		7.8	7.6	7.7	**0.28**
Spring to North of Deep Dbl concrete tubs	9	7.55	7.55	7.54	7.60	7.62		7.6	7.6	7.6	**0.08**
Parisol Pool (next to river)	10	7.13	7.13	7.12	7.27	7.31		7.2	7.2	7.2	**0.19**
By the Rock Pool	11	7.19	7.19	7.13	7.26	7.25		7.2	7.2	7.2	**0.13**
Pool Above "By the Rock"	12	7.56	7.56	7.50	7.78	7.57		7.5	7.7	7.6	**0.28**
Little Tufa Mound Spring Box	13	7.14	7.14	7.09	7.09	7.60		7.3	7.1	7.2	**0.51**
											0.23

Spring	#	16-Jun-11	14-Oct-11	5-Jun-12	20-Sep-12	7-Jun-13	30-Sep-13	Fall Mean	Spring Mean	Ave. pH	Range Diff.
Roadside Pool (above Little Eden)	2	7.5	7.5	7.5	7.5	7.48	7.65	7.5	7.5	7.5	**0.17**
Little Eden	3	7.8	7.7	7.7	7.6	7.93	7.95	7.7	7.8	7.8	**0.35**
Double Concrete Tub (@ base of Tufa Hill)	4	7.3	7.3	7.2	7.3	7.3	7.36	7.3	7.3	7.3	**0.13**
Spring Box @ top of Tufa Hill	6	7.2	n/s	n/s	7.4	7.15	7.33	7.4	7.2	7.3	**0.25**
Deep Double Concrete Tubs	7	7.5	7.5	7.6	7.5	7.56	7.64	7.6	7.6	7.6	**0.11**
Spring by Board Bridge (to Deep Dbl tubs)	8	7.5	7.8	7.6	8.0	7.6	7.79	7.9	7.6	7.7	**0.46**
Spring to North of Deep Dbl concrete tubs	9	7.4	7.4	7.7	7.5	7.65	7.85	7.6	7.6	7.6	**0.47**
Parisol Pool (next to river)	10	ns	7.4	7.5	7.4	7.26	7.36	7.4	7.4	7.4	**0.20**
By the Rock Pool	11	7.5	7.3	7.5	7.5	7.36	7.49	7.4	7.5	7.4	**0.13**
Pool Above "By the Rock"	12	7.6	7.7	7.7	7.6	7.68	7.93	7.7	7.7	7.7	**0.35**
Little Tufa Mound Spring Box	13	7.3	7.6	n/s	n/s	7.28	7.37	7.5	7.3	7.4	**0.09**

term pH trend described earlier, there appears to be no coherent seasonal fluctuation in thermal spring pH values (Table 4).

A review of studies providing pH information for thermal springs in the vicinity of Mono Hot Springs provides context for understanding the findings described above. Feth et al. (1964) conducted a broad study of chemical content in natural water in the Sierra Nevada. Water samples were collected within the batholithic rocks of the Sierra Nevada from south of Visalia, California, north to near Downieville, California (Feth et al., 1964, plate 1). Their sampling points included eight thermal springs in granitic rock exclusive of the ones in this study. Their field pH values for these thermal springs ranged from 7.0 to 9.4, with a mean of 8.6. The pH values measured at Mono Hot Springs, which rises through Mount Givens Granodiorite, falls within Feth's range of thermal spring pH values. The pH of the Blayney Meadows (Muir Trail Ranch) thermal spring in 2015 was 8.68, compared to the 8.0 during monitoring in 1974 (Mariner et al., 1977), and is also within the pH range found during the study of natural water in the Sierra Nevada (Feth et al., 1964). In contrast, the only spring found flowing within the travertine deposits near Mono Crossing in 2013 had a pH of 6.4, which is just outside the range of the thermal spring pH values determined by Feth and others (1964) and significantly less than their mean value. The long-term pH increase at Blayney Meadow Hot Spring mirrors that seen at Mono Hot Springs during the current study.

ANALYSIS OF THERMAL SPRING SOURCE

We chose a subset of Mono Hot Springs for geothermometer analysis. The thermal springs selected for sampling included spring 6, with the highest temperatures and most consistent temperature; spring 7, which is also consistent, but at a notably lower temperature; spring 8, which displays the most variable temperatures annually; and spring 12, which also shows significant annual variability in temperature and consistently has the lowest temperature (Table 1 and Figure 2A).

The calculated rock-water equilibration temperatures for Mono Hot Springs water is between 70 and 79°C using the two cation geothermometers (Table 5). Estimating temperature at depth by this means is a standard approach in geothermal exploration (e.g., Williams et al., 2008). The values computed by any chemical or isotopic geothermometers rest on the key

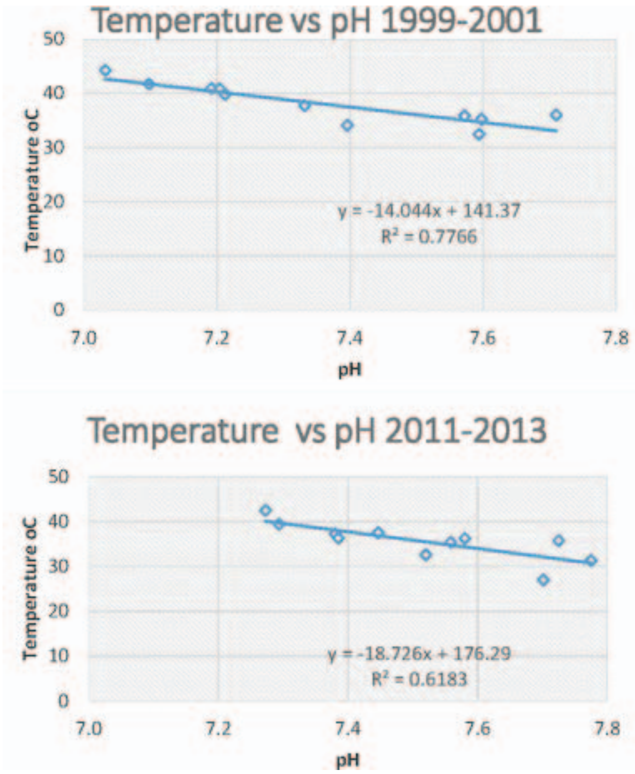

Figure 6. Graphs showing the relationship between pH and average annual temperature for both the initial and later monitoring periods. The formula on each graph is the regression expressing this relationship.

assumption that fluid composition is not changed during its ascent from the hot source aquifer to the spring. Additionally, it is assumed that there are chemical equilibria for the relevant cations within that source aquifer (D'Amore and Arnórsson, 1990). If either of these assumptions is violated, the temperatures of 70–79°C for these four springs may not be the hottest temperature for the heat source but would instead represent a minimum temperature. For springs 6, 7, 8, and 12, the heat source temperature calculated from both cation geothermometers is about twice the temperature of water emerging at the surface. Mariner and others (1977) computed a source temperature in their 1974 sample of 80°C for spring 6 using the Na-K-Ca geothermometer, which compares well to our 79°C (Table 5).

Table 5 also shows the source temperature varying from 105 to 109°C, using the silica geothermometer for springs 6, 7, 8 and 12. These temperature values are about 25 to 30°C greater than those computed using the cation geothermometers, suggesting an overestimation of the heat source temperature. With silica geothermometers, reactions can change the silica content to produce this effect. D'Amore and Arnórsson (1990) note that boiling is one way this increase in aqueous silica within the hot water can happen. Another means for increasing silica concentration is through dilution and mixing with cooler water from shallow aquifers (Kolesar and De Graff, 1978; Oerter, 2011). Given that our emerging waters at Mono Hot Springs are less than the 100°C necessary for boiling, and given that shallow groundwater in the region is known to increase in silica content during snowmelt recharge (Feth et al., 1964), dilution by shallow groundwater seems a likely mechanism for this proposed overestimation of source temperature. Mariner and others (1977) obtained a silica geothermometer–based source temperature of 110°C for spring 6. They attributed this higher value to dilution with high-silica surface water from a creek upslope of spring 6. Our geothermometry results for spring 6 were consistent with those obtained in 1974 (Mariner et al., 1977). Our cation and silica geothermometer differences at spring 6 are mirrored at springs 7, 8, and#12, despite their physical location being some distance from spring 6 and despite the differing physical characteristics (distance from river, elevation, pool within native soil vs. concrete walls). Based on these findings, it seems reasonable to conclude that mixing of shallow cooler groundwater with rising thermal water is more likely the rule rather than the exception. Our data establish that despite having different average annual temperatures and seasonal temperature variability, thermal springs existing in the Mono Hot Springs area have a source with a similar temperature at depth.

Table 5. *Geothermometer results. Data for each of the springs sampled includes instantaneous temperature of each thermal spring sampled for geothermometry, computed heat source temperature for the two cation geothermometers and the silica geothermometer, and average thermal spring temperature for the later monitoring period, when the sampling took place. Each spring is represented on Figure 3A and shown in Figure 4.*

Spring No.	Sampled Temperature (°C)	Na-K-Ca (°C)	K-Mg (°C)	Silica (°C)	Average Thermal Spring Temperature (°C)*
6: Spring box on tufa hill	43.7	79	74	106	43
7: Double deep concrete tubs at base of tufa hill	42.3	79	74	107	35
8: Spring by board bridge	38.8	74	74	109	36
12: Pool upslope from spring 11	29.8	74	70	105	27

*Calculated from the samples taken during the later monitoring period (2011–2013).

DISCUSSION

As noted earlier, Mono Hot Springs is one of several thermal spring localities along the valley bottom of the South Fork of the San Joaquin River. The chemistry of thermal springs of the Sierra Nevada in general (Feth and others, 1964) and of Mono Hot Springs and Blayney Meadow Hot Spring, specifically (Mariner et al., 1977), indicates outflow reflective of deep circulation by meteoric water. Although Lockwood and others (1972) indicate that thermal springs are present along the South Fork of the San Joaquin for a distance of about 19 km downstream from Mono Hot Springs, their map only shows one spring in the vicinity of Crater Lake Meadow and the one at Mono Crossing. Blayney Meadow Hot Spring, including the one at Muir Trail Ranch, lies 18 km upstream from Mono Hot Springs. We note that these four localities—Crater Lake Meadow, Mono Crossing, Mono Hot Springs, and Blayney Meadow—form a linear array (Figures 1 and 2), though this corresponds to the orientation of the San Joaquin River South Fork. Only two known locations, Mono Crossing Hot Spring and Mono Hot Springs, have extensive deposits. It is reasonable to assume that thermal water was rising at these locations at least since the retreat of glacial ice from this area at about 15 ka (Phillips, 2016) to create the extensive travertine terraces near Mono Crossing and the tufa mounds at Mono Hot Springs. The nature of these deposits makes them unlikely to have survived being overridden by glacial ice. The thermal springs downstream from Mono Crossing Hot Springs are described by Lockwood and others (1972) as being cooler than Mono Hot Springs. However, the National Oceanic and Atmospheric Administration hot springs database provides a temperature of 35°C for the Crater Lake Meadow thermal spring, while Mono Crossing thermal spring was 18.2°C when we measured it on June 6, 2013. The extensive travertine deposits at Mono Crossing indicate a higher temperature in the past, given their comparison to the Mammoth Hot Springs in Yellowstone Park (Bargar, 1978). This suggests some significant change to the thermal water paths to Mono Crossing. Mono Hot Springs and the Blayney Meadow (Muir Trail Ranch) Hot Spring have comparable higher temperatures of about 44°C. We currently have insufficient data to explain the wide differences in South Fork San Joaquin thermal spring temperatures. Variable dilution by shallow aquifers and/or independent geothermal systems could separately or together account for the variability.

What is the nature of the geothermal heat source at Mono Hot Springs? Certainly, thermal springs are often related to magma bodies at depth, as exemplified by those present in Yellowstone National Park (Bargar, 1978). Remnants of Pliocene flows of trachybasalt are found along much of the South Fork of the San Joaquin River valley (Figure 2B) (Bateman, 1965; Bateman et al., 1971; and Lockwood and Lydon, 1975). Devil's Table, an example of one of these remnants, is less than 2 km north-northwest of Mono Hot Springs. Mariner and others (1977) suggested that the proximity of these flows to Mono Hot Springs might indicate a magmatic heat source, but their age (Manley et al., 2000) makes it unlikely that this or related intrusions continue to warm the area. Any magmatic heating of the Mono Hot Springs water would have to be from more recent or ongoing intrusions.

Conductive heating through thinned lithosphere, while insufficient without fracture porosity, may contribute to thermal springs in the vicinity of the study area. Ducea and Saleeby (1996, 1998) demonstrated that lithosphere in the study area thinned during the Neogene by delamination and has been replaced by (warmer) asthenosphere. Today, lithosphere in the study area is 35–45 km thick (Frassetto et al., 2011), similar to the distance from Mono Hot Springs to the east edge of the Sierra Nevada microplate (Figure 1). However, reduced heat flow in the area is low (Saltus and Lachenbruch, 1991), and warming from hypothesized replacement of the Sierran root with warm asthenosphere will not have reached the surface yet, if purely by conduction (Brady et al., 2006).

The proximity of Mono Hot Springs to the active faults within Walker Lane, Long Valley Caldera, and Mammoth Mountain suggests a possible relationship to these large-scale features (Faulds et al., 2004). Mammoth Mountain and the Long Valley geothermal systems are the largest most-proximal possible influences. These systems include geothermal waters in excess of 200°C that are clearly being heated by magma at depth (Hilton, 1996; Sorey et al., 2000). The likely presence of a magma body (Stroujkova and Malin, 2000), continuing probable diking (Hill and Prejean, 2005; Templeton and Dreger, 2006), and the large number of active and extinct thermal spring features (Berry et al., 1980; Sorey et al., 2000) in Long Valley highlight the substantial heat input there. However, the ~30-km distance between Long Valley or Mammoth Mountain and Mono Hot Springs reduces the likelihood of direct flow of water between them and the study area. What seems more likely is that related tectonic effects exist within the study area.

Significant small-magnitude seismicity occurs within the Sierra Nevada around the Long Valley Caldera (Figure 2A and ANSS Comprehensive Earthquake Catalog). A concentration of epicenters forms a cluster between Long Valley and Mono Hot Springs, as well as a large concentration north of Blayney Meadow (Figure 2A). The seismicity trend between Long

Valley and Mono Hot Springs passes through Mammoth Mountain, the Fish Creek/Iva Bel Hot spring, and unnamed Quaternary active normal faults near Mammoth (USGS, 2017). This low-magnitude (M 2–3) seismicity is mostly shallow (<10 km in depth) and exhibits dominantly normal fault focal mechanisms mostly oriented subparallel to this hypothesized lineament (Figures 1 and 2A). The proposed feature, composed of mapped faults, seismicity, and thermal springs, is subparallel to known left-stepping north-south–oriented normal faults, such as the Hilton Creek Fault (Figure 1), that accommodate NNW-oriented dextral shear in the area (Unruh et al., 2003). Such faults are consistent with formation under dextral trans-tension in this part of the eastern Sierra Nevada (Unruh et al., 2003). In a trans-tensional setting, this faulting and seismicity would likely produce porosity and geothermal fluid-flow pathways and might also include dike emplacement. We speculate that at a minimum, this seismicity indicates one or more faults that permit deep circulation of thermal water to Mono Hot Springs.

Seismicity also has the potential to affect the flow paths of rising thermal water in ways that might alter their flow rate or temperature (e.g., Wang et al., 2004; City of El Paso de Robles, 2007). The Blayney Meadow (Muir Trail Ranch) spring located within the John Muir Wilderness provides insight on this potential impact due to an observed earthquake event. The thermal spring at Muir Trail Ranch, on a private land holding at Blayney Meadow within the John Muir Wilderness (Sierra National Forest), was affected by an earthquake in the 1990s. Unfortunately, the date and time were not recorded for this event. Because of the operation of the Ranch, it would have taken place between June and September. Witnesses recalled the earthquake to have probably occurred in late morning or midday sometime in July (H. Painter, Muir Trail Ranch, written comm., 2015). After the earthquake shaking ceased, reports indicate that the spring had stopped flowing. Shortly afterwards, it restarted in spurts for nearly an hour before resuming a continuous flow. However, the flow for the remainder of the day was a cloudy gray color (H. Painter, Muir Trail Ranch, written comm., 2015). The thermal spring flowed normally the following day. No other change, such as temperature change, was noted. However, precise temperature measurement of this spring is only limited to the 1974 sample reported in Mariner and others (1977) and our 2015 sample.

The lack of impact to the spring's temperature from the 1990s earthquake is even more important because of the severe shaking sustained by this area on May 25, 1980. Three earthquakes on the Hilton Creek Fault near Mammoth Lakes, California (of magnitude 6.2, 5.0, and 5.9), took place between 8:33 AM and 11:44 AM (Stover and Coffman, 1993). The shaking would have affected both the Blayney Meadow (Muir Trail Ranch) and Mono Hot Springs areas. Yet the temperatures taken by Mariner and others (1977) during their 1974 field work and those we took in 2015 at Muir Trail Ranch and those taken at Mono Hot Spring 6 during our monitoring do not reflect any persistent temperature change. There are no records of any short-term effects from the May 1980 earthquakes, such as those reported for the thermal spring at Muir Trail Ranch, because they occurred prior to the seasonal occupancy of the area. This was likely the case also for observable short-term effects at any of the thermal springs in the Mono Hot Springs area, because the snow blocking Kaiser Pass Road prevented site access at that time. In order to robustly investigate effects of seismicity on thermal water temperature in the area, regular monitoring would be necessary. Nonetheless, the observations outlined here appear to indicate that earthquakes during the study period did not alter the temperature of thermal water issuing from either Mono Hot Springs or the hot springs at Blayney Meadow.

Current monitoring data for Mono Hot Springs demonstrate a slight cooling trend of ~2 to 3°C over the decade between the initial and later monitoring periods (Figure 6), though some springs seem more stable than that. Data from 1974 indicate a temperature of 43°C for spring 6 (Mariner et al, 1977), slightly lower than that of the 1999–2001 monitoring period and identical to its temperature during the 2011–2013 monitoring period. Similarly, temperatures at one of the thermal springs at Blayney Meadow (Muir Trail Ranch) upstream from Mono Hot Springs was also stable between 1974 (43°C; Mariner et al., 1977) and our monitoring on July 16, 2015 (42.4°C). The stability of temperatures at the hottest springs (Mono Hot Spring 6 and Blayney Meadow/Muir Trail Ranch) over three decades (1974–2015) compared to the decade-long trend of about 2 to 3°C cooling for the group of Mono Hot Springs suggests other possibilities.

Differences in near-surface mixing with meteoric waters may be a cause, as could changes in the near-surface flow paths of the lower-temperature springs. The dormancy or extinction of activity at some Mono Crossing thermal spring features clearly signals temporal variability at that locality as well. Robust conclusions about the temporal evolution of the thermal springs in the study area await continued monitoring through seismicity, changes in surface water availability (e.g., drought), and other uncontrolled variability.

Shallow cooler groundwater is more available in the springtime after snowmelt, based on surface observations. Yet thermal spring temperatures are higher during springtime than during fall after the long, dry summer. This apparent contradiction suggests that increased deep groundwater flow occurs due to seasonal-runoff–triggered aquifer pressure changes. Testing this hypothesis would likely require flow data for the thermal springs during spring and fall. At this time, flow data on spring 6 taken at the time of sampling in 1974 are the only data available (Mariner et al., 1977). While understanding how the Mono Hot Springs are influenced by groundwater circulation in the surrounding aquifer is desirable, it is outside the scope of this initial study.

CONCLUSIONS

Our findings show that the individual springs at Mono Hot Springs display consistent temperature and pH relationships seasonally and over multiple years. Primary control is exerted by heating at depth and groundwater flow through underground conduits. As guidance for management of this natural resource, passive catchment of the thermal spring outflow for recreational uses is unlikely to alter these relationships. Consequently, the attributes of the springs that have sustained Native American spiritual values should persist under such current uses. Management actions that might introduce additional surface water into the thermal spring area, such as modifying existing road drainage, should be avoided, as additional surface water mixing could decrease some thermal spring temperatures. Similarly, drilling wells and pumping water from within the spring area or affecting the conduits along which hot water rises obviously could alter the thermal spring conditions.

An important aspect of managing a natural resource is understanding how, or if, it varies over time and what factors influence this normal variability. Such basic data enable a better analysis of how management action may or may not alter the natural operation of the resource. In the case of Mono Hot Springs, we needed to understand the thermal character of the springs. The springs in the Mono Hot Springs area are now known to range in temperature from a high of 44.5°C to a low of 24.3°C and from a pH of 8.0 to 7.05. Some springs display a very consistent annual temperature and others show significant variability. The decade between periods of data gathering showed a 2 to 3°C decrease in average thermal spring temperatures and an increase in pH. However, this trend may only be a minor variation because this decade falls within the three-decade trend, represented by Mono Hot Spring 6 and Blayney Meadow (Muir Trail Ranch) hot spring, showing a constant temperature trend. Both data-gathering periods detected a statistically verified seasonal (late spring vs. early fall) difference in the temperatures, but not in pH. Because the temperature variability is in the water outflow from the springs, the mixing of shallow cooler groundwater with rising thermal water seems a likely mechanism.

Combined data sets suggest that the Mono Hot Springs may be caused by tectonic activity along a minor fault system within the Sierra Nevada Microplate. Mapped Quaternary active normal faults and earthquake epicenters with dominantly normal-fault focal mechanisms coincide along a lineament that includes geothermal activity at Mammoth Mountain, Fish Creek/Iva Bell Hot Spring, and Mono Hot Springs (Figures 1 and 2A).

Finally, assuming water-rock equilibrium, the temperature of the heat source generating these thermal springs is at least 74–79°C. The temperatures computed using cation geothermometers produced the same source temperature for one of the sampled springs as an investigation by the U.S. Geological Survey conducted 39 years earlier. The difference in calculated heat source temperature between cation and silica geothermometers is indicative of shallow groundwater mixing with rising hot water before flowing from the thermal springs. The pathways permitting meteoric water to circulate at depth to this heat source can be temporarily impacted by earthquake activity and shaking. However, the Blayney Meadow (Muir Trail Ranch) spring observation described above suggests that changes only last a few days at most.

Future monitoring in support of land management decision-making should not be limited to only one or two springs. The 1974 sampling of Mono Hot Spring 6 provided a valuable snapshot at that time. However, the monitoring of 11 springs in this study demonstrates the more comprehensive understanding of spring conditions made possible with a larger data set drawn over a longer monitoring period. Any future monitoring should take into account the seasonal differences detected and provide a means for continuing assessment of long-term temperature trends. Given the lack of data on flow rates from the springs, collecting flow data might provide valuable information to add to the temperature and pH data.

ACKNOWLEDGMENTS

The manuscript substantially benefited from reviews by Allen Glazner, Elizabeth Haddon, and an anonymous reviewer.

REFERENCES

Argus, D. F. and Gordon, R. G., 1991, Current Sierra Nevada–North America motion from very long baseline interferometry: Implications for the kinematics of the western United States: *Geology*, Vol. 19, pp. 1085–1088.

Argus, D. F. and Gordon, R. G., 2001, Present tectonic motion across the Coast Ranges and San Andreas fault system in

Central California: *Geological Society America Bulletin*, Vol. 113, No. 12, pp. 1580–1592.

Bacon, C. R.; Giovannetti, D. M.; Duffield, W. A.; Dalrymple, G. B.; and Drake, R. E., 1982, *Age of the Coso Formation, Inyo County, California*: U.S. Geological Survey Bulletin 1527, 18 p.

Bailey, R. A., 1989, *Geologic Map of Long Valley Caldera, Mono-Inyo Craters Volcanic Chain, and Vicinity, Eastern California*: U.S. Geological Survey Miscellaneous Investigations Map I-1933, scale 1:62,500, p. 11.

Bargar, K. E., 1978, *Geology and Thermal History of Mammoth Hot Springs, Yellowstone National Park, Wyoming*: U.S. Geological Survey Bulletin 1444, 55 p.

Bateman, P. C., 1965, *Geologic Map of the Blackcap Mountain Quadrangle, Fresno County, California*: U.S. Geological Survey Geologic Quadrangle Map GQ-428.

Bateman, P. C.; Lockwood, J. P.; and Lydon, P. A., 1971, *Geologic Map of the Kaiser Peak Quadrangle, Central Sierra Nevada, California*: U.S. Geological Survey Geologic Quadrangle Map GQ-894.

Berg, N. H.; Gallegos, A.; Dell, T., Frazier, J.; Procter, T.; Sickman, J.; and Arbaugh, M., 2005, A screening procedure for identifying acid-sensitive lakes from catchment characteristics: *Environmental Monitoring Assessment*, Vol. 105, No. 1–3, pp. 285–307.

Berry, G. W.; Grim, P. J.; and Ikelman, J. A., 1980, *Thermal Spring List for the United States*: National Oceanic and Atmospheric Administration Key to Geophysical Records Documentation No. 12, 59 p.

Brady, R. J.; Ducea, M. N.; Kidder, S. B.. and Saleeby, J. B., 2006, The distribution of radiogenic heat production as a function of depth in the Sierra Nevada Batholith, California: *Lithos*, Vol. 86, No. 3, pp. 229–244.

Brossy, C. C.; Kelson, K. I.; Amos, C. B.; Baldwin, J. N.; Kozlowicz, B.; Simpson, D.; Ticci, M. G.; Lutz, A. T.; Kozaci, O.; Streig, A.; Turner, R.; and Rose, R., 2012, Map of the late Quaternary active Kern Canyon and Breckenridge faults, southern Sierra Nevada, California: *Geosphere*, Vol. 8, No. 3, pp. 581–591, 511.

Cheeney, R. F., 1983, *Statistical Methods in Geology for Field and Lab Decisions*: George Allen & Unwin, London, U.K. 169 p.

City of El Paso de Robles, 2007, *Supplemental Environmental Assessment to the Programmatic Environmental Assessment (PEA) for Typical Recurring Actions Resulting from Flood, Earthquake, Fire, Rain, and Wind Disasters in California as Proposed by the Federal Emergency Management Agency, FEMA-1505-DR-CA*: Electronic document, available at https://www.fema.gov/media-library-data/20130726-1609-20490-1143/pasoroblescityhall_sea.txt

CSBSJU, 2016, *Kolmogorov-Smirnov Test, Department of Physics, College of Saint Benedict Saint John's University,* Minnesota: Electronic document, available at http://www.physics.csbsju.edu/stats/KS-test.html

D'Amore, F. and Arnórsson, S., 2000, Geothermometry. In Arnórsson, S. (Editor), *Isotopic and Chemical Techniques in Geothermal Exploration, Development, and Use*: International Atomic Energy Agency, Vienna, Austria, pp. 152–199.

De Graff, J. V., 1979, Initiation of shallow mass movement by vegetative-type conversion: *Geology*, Vol. 7, pp. 426–429.

De Graff, J. V., 1982, An approach for avoiding damage to springs from shock waves generated during seismic exploration. In Nielson, D. L.(Editor), *Overthrust Belt of Utah*: Utah Geological Association Publication 10, pp. 163–166.

De Graff, J. V., 2011, Perspectives for systematic landslide monitoring: *Environmental Engineering Geoscience*, Vol. 17, No. 1, pp. 67–76.

De Graff, J. V. and Gallegos, A. J., 1987, Measuring soil loss to address erosion control needs in natural resources management. In *Proceedings of the International Erosion Control Association*, Annual Meeting, Sparks, NV, pp. 267–276.

De Graff, J. V.; Gallegos, A. J.; Reid, M. E.; LaHusen, R. G.; and Denlinger, R. P., 2015, Using monitoring and modeling to define the hazard posed by the reactivated Ferguson rock slide, Merced Canyon, California: *Natural Hazards*, Vol. 76, No. 2, pp. 769–789.

De Graff, J. V.; Roath, B.; and Franks, E., 2007, Monitoring to improve the understanding of herbicide fate and transport in the southern Sierra Nevada, California. In Furniss, M.; Clifton, C.; and Ronnenberg, K. (Editors), *Advancing the Fundamental Sciences: Proceedings of the Forest Service National Earth Sciences Conference*: San Diego, CA, October 18–22, 2004, PNW-GTR-689, Pacific Northwest Research Station, USDA Forest Service, Portland, OR, Vol. 2, pp. 352–360.

De Graff, J. V. and Romesburg, H. C., 1981, Subsidence crack closures: Rate, magnitude, and sequence: *Bulletin International Association Engineering Geology*, No. 23, pp. 123–127.

Dixon, T. H.; Miller, M.; Farina, F.; Wang, H.; and Johnson, D., 2000, Present-day motion of the Sierra Nevada block and some tectonic implications for the Basin and Range province, North American Cordillera: *Tectonics*, Vol. 19, No. 1, pp. 1–24.

Dixon, T. H.; Robaudo, S.; Lee, J.; and Reheis, M. C., 1995, Constraints on present-day Basin and Range deformation from space geodesy: *Tectonics*, Vol. 14, No. 4, pp. 755–772.

Dong, S.; Ucarkus, G.; Wesnousky, S.; Maloney, J.; Kent, G.; Driscoll, N.; and Baskin, R.; 2014, Strike-slip faulting along the Wassuk Range of the northern Walker Lane, Nevada: *Geosphere*, Vol. 10, No. 1, pp. 40–48.

Ducea, M. and Saleeby, J. B., 1998, A case for delamination of the deep batholithic crust beneath the Sierra Nevada, California: *International Geology Review*, Vol. 40, No. 1, pp. 78–93.

Ducea, M. N. and Saleeby, J. B., 1996, Buoyancy sources for a large, unrooted mountain range, the Sierra Nevada, California; Evidence from xenolith thermobarometry: *Journal Geophysical Research*, Vol. 101, No. B4, pp. 8229–8244.

Farmer, G. L.; Glazner, A. F.; and Manley, C. R., 2002, Did lithospheric delamination trigger late Cenozoic potassic volcanism in the southern Sierra Nevada, California?: *Geological Society America Bulletin*, Vol. 114, No. 6, pp. 754–768.

Faulds, J. E.; Coolbaugh, M.; Blewitt, G.; and Henry, C. D., 2004, Why is Nevada in Hot Water? Structural controls and tectonic model of geothermal systems in the northwestern Great Basin: *Geothermal Resources Council Transactions*, Vol. 28, pp. 649–654.

Feth, J. H.; Rogers, S. M.; and Roberson, C. E., 1964, *Chemical Composition of Snows in the Northern Sierra Nevada and Other Areas*: U.S. Geological Survey Water-Supply Paper 1535.

Forest History Society, 2009, *Introduction: Managing Multiple Uses on National Forests, 1905–1995*: Electronic document, available at http://www.foresthistory.org/ASPNET/Publications/multiple_use/chap1.htm

Fournier, R. O., 1977, Chemical geothermometers and mixing models for geothermal systems: *Geothermics*, Vol. 5, pp. 41–50.

Fournier, R. O. and Truesdall, A. H., 1973, An empirical Na-K-Ca geothermometer for natural waters: *Geochimica Cosmochimica Acta*, Vol. 37, pp. 1255–1275.

Frassetto, A. M.; Żandt, G.; Gilbert, H.; Owens, T. J.; and Jones, C. H., 2011, Structure of the Sierra Nevada from receiver functions and implications for lithospheric foundering: *Geosphere*, Vol. 7, No. 4, pp. 898–921.

Frazer, R. E.; Coleman, D. S.; and Mills, R. D., 2014, Zircon U-Pb geochronology of the Mount Givens Granodiorite:

Implications for the genesis of large volumes of eruptible magma: *Journal Geophysical Research: Solid Earth*, Vol. 119, No. 4, pp. 2907–2924.

Giggenbach, G. F., 1988, Geothermal solute equilibria: *Geochimica Cosmochimica Acta*, Vol. 52, pp. 2749–2765.

Hildreth, W. and Fierstein, J., 2016, *Eruptive History of Mammoth Mountain and its Mafic Periphery, California*: U.S. Geological Survey Professional Paper 1812, 128 p.

Hildreth, W.; Fierstein, J.; Champion, D.; and Calvert, A., 2014, Mammoth Mountain and its mafic periphery—A late Quaternary volcanic field in eastern California: *Geosphere*, Vol. 10, No. 6, pp. 1315–1365.

Hill, D. P. and Prejean, S., 2005, Magmatic unrest beneath mammoth mountain, California: *Journal Volcanology Geothermal Research*, Vol. 146, No. 4, pp. 257–283.

Hilton, D. R., 1996, The helium and carbon isotope systematics of a continental geothermal system: Results from monitoring studies at Long Valley caldera (California, USA): *Chemical Geology*, Vol. 127, No. 4, pp. 269–295.

Jager, H. I. and Rose, K. A., 2003, Designing optimum flow patterns for fall Chinook Salmon in a Central Valley, California river: *North American Journal Fisheries Management*, Vol. 23, pp. 1–21.

Jones, C. H.; Lang Farmer, G.; and Unruh, J., 2004, Tectonics of Pliocene removal of lithosphere of the Sierra Nevada, California: *Geological Society America Bulletin*, Vol. 116, No. 11–12, pp. 1408–1422.

Kolesar, P. T. and De Graff, J. V., 1978, A comparison of the silica and Na-K-Ca geothermometers for thermal springs in Utah: *Geothermics*, Vol. 6, pp. 221–226.

Kreemer, C.; Blewitt, G.; and Hammond, W. C., 2009, Geodetic constraints on contemporary deformation in the northern Walker Lane: 2. Velocity and strain rate tensor analysis. In Oldow, J. S. and Cashman, P. H. (Editors), *Late Cenozoic Structure and Evolution of the Great Basin-Sierra Nevada Transition*, Volume 447, Geological Society of America, Boulder, CO. pp. 17–31.

Langbein, J. O.; Hill, D. P.; Parker, T. N.; and Wilkinson, S. K., 1993, An episode of reinflation of the Long Valley Caldera, eastern California; 1989–1991: *Journal Geophysical Research*, Vol. 98, No. B9, pp. 15851–15870.

Lockwood, J. P.; Bateman, P. C.; and Sullivan, J. S., 1972, *Mineral Resource Evaluation of the U.S. Forest Service Sierra Demonstration Project Area, Sierra National Forest, California*: U.S. Geological Survey Professional Paper 714, 30 p.

Lockwood, J. P. and Lydon, P. A., 1975, *Geologic Map of the Mount Abbot Quadrangle, Central Sierra Nevada, California*: U.S. Geological Survey Geologic Quadrangle Map GQ-1155.

Mammoth Pacific, 2017, *Welcome to the Mammoth Geothermal Complex Website*: Electronic document, available at http://www.mammothpacific.com/

Manley, C. R.; Glazner, A. F.; and Farmer, G. L., 2000, Timing of volcanism in the Sierra Nevada of California; Evidence for Pliocene delamination of the batholithic root?: *Geology*, Vol. 28, No. 9, pp. 811–814.

Mariner, R. H.; Presser, E. S.; and Evans W. C., 1977, *Hot Springs of the Central Sierra Nevada, California*: U.S. Geological Survey Open-File Report 77-559, 27 p.

Monastero, F. C., 2002, Model for success: An overview of industry-military cooperation in the development of power operations at the Coso Geothermal Field in Southern California: *Geothermal Resources Council Bulletin*, Vol. 31, No. 5, pp. 188–195.

Moore, J. G. and Sisson, T. W., 1985, *Geologic Map of the Kern Peak Quadrangle, Tulare County, California*: U.S. Geological Survey, Reston, VA, p. 1 sheet.

National Centers for Environmental Information (NCEI), *Thermal Springs in the US*: Electronic document, available at https://maps.ngdc.noaa.gov/viewers/hot_springs/, National Ocean and Atmospheric Administration.

Neuendorf, K. K. E.; Mehl, J. P. Jr.; and Jackson, J. A. (Editors), 2011, *Glossary of Geology, Fifth Edition, Revised*: American Geosciences Institute, Alexandria, VA.

Oerter, E. J., 2011, *Geothermometry of Thermal Springs in the Rico, Dunton, and West Fork Dolores River Areas, Dolores County, Colorado*: Colorado Geological Survey, Denver, CO, 56 p.

Oldow, J. S.; Geissman, J. W.; and Stockli, D. F., 2008, Evolution and strain reorganization within late Neogene structural stepovers linking the central Walker Lane and northern Eastern California shear zone, western Great Basin: *International Geology Review*, Vol. 50, No. 3, pp. 270–290.

Phillips, F. M., 2016, Cosmogenic nuclide data sets from the Sierra Nevada, California, for assessment of nuclide production models: I. Late Pleistocene glacial chronology: *Quaternary Geomorphology*, Vol. 35, pp. 119–129.

Rose, G., 1994, *Sierra Centennial*: Three Forest Interpretative Association, Auberry, CA. 183 p.

Saltus, R. W. and Lachenbruch, A. H., 1991, Thermal evolution of the Sierra Nevada; Tectonic implications of new heat flow data: *Tectonics*, Vol. 10, No. 2, pp. 325–344.

Sarna-Wojcicki, A. M.; Pringle, M. S.; and Wijbrans, J., 2000, New (super 40) Ar/(super 39) Ar age of the Bishop Tuff from multiple sites and sediment rate calibration for the Matuyama-Brunhes boundary: *Journal Geophysical Research*, Vol. 105, No. B9, p. 21.

Sierra Nevada Geotourism, 2017, *Southern California Edison Big Creek Hydroelectric Project*: Electronic document, available at https://www.sierranevadageotourism.org/content/southern-california-edison-big-creek-hydroelectric-project/sie5ee9ccaf96c262c3c

Sorey, M. L.; Farrar, C. D.; Gerlach, T. M.; McGee, K. A.; Evans, W. C.; Colvard, E. M.; Hill, D. P.; Bailey, R. A.; Rogie, J. D.; Hendley, J. W., II; and Stauffer, P. H., 2000, *Invisible CO_2 Gas Killing Trees at Mammoth Mountain, California: Fact Sheet 172-96 (Version 2.0)*: U.S. Geological Survey, 2 p.

Surpless, B. E.; Stockli, D. F.; Dumitru, T. A.; and Miller, E. L., 2002, Two-phase westward encroachment of Basin and Range extension into the northern Sierra Nevada: *Tectonics*, Vol. 21, No. 1, pp. 2-1-2-10.

Templeton, D. C. and Dreger, D. S., 2006, Non-double-couple earthquakes in the Long Valley Volcanic Region: *Bulletin Seismological Society America*, Vol. 96, No. 1, pp. 69–79.

Tobisch, O. T.; Saleeby, J. B.; Renne, P. R.; McNulty, B.; and Tong, W., 1995, Variations in deformation fields during development of a large-volume magmatic arc, central Sierra Nevada, California: *Geological Society America Bulletin*, Vol. 107, No. 2, pp. 148–166.

Unruh, J. and Hauksson, E., 2009, Seismotectonics of an evolving intracontinental plate boundary, southeastern California. In Oldow, J. S. and Cashman, P. H. (Editors), *Late Cenozoic Structure and Evolution of the Great Basin–Sierra Nevada Transition*: Geological Society of America Special Paper 447, pp. 351–372.

Unruh, J.; Hauksson, E.; and Jones, C. H., 2014, Internal deformation of the Southern Sierra Nevada Microplate associated with foundering lower lithosphere, California: *Geosphere*, Vol. 10, No. 1, pp. 107–128.

Unruh, J.; Humphrey, J.; and Barron, A., 2003, Transtensional model for the Sierra Nevada frontal fault system, eastern California: *Geology*, Vol. 31, No. 4, pp. 327–330.

U.S. Geological Survey (USGS) and California Geological Survey (GSC), 2006, *Quaternary Fault and Fold Database for the United States: U.S. Geological Survey Web Site*: Electronic document, available at http//earthquake.usgs.gov/hazards/qfaults/

USGS, 2017, *Advanced National Seismic System (ANSS) Comprehensive Earthquake Catalog (ComCat): U.S. Geological Survey*: Electronic document, available at https://earthquake.usgs.gov/earthquakes/

Wakabayashi, J. and Sawyer, T. L., 2000, Neotectonics of the Sierra Nevada and the Sierra Nevada-Basin and Range transition, California, with field trip stop descriptions for the northeastern Sierra Nevada. In Brooks, E. R. and Dida, L. T. (Editors), *Field Guide to the Geology and Tectonics of the Northern Sierra Nevada*: California Division of Mines and Geology Special Publication 122, pp. 173–212.

Wakabayashi, J. and Sawyer, T. L., 2001, Stream incision, tectonics, uplift, and evolution of topography of the Sierra Nevada, California: *Journal Geology*, Vol. 109, No. 5, pp. 539–562.

Wang, C. Y.; Manga, M.; Dreger, D.; and Wong, A., 2004, Streamflow increase due to rupturing of hydrothermal reservoirs: Evidence from the 2003 San Simeon, California, Earthquake: *Geophysical Research Letters*, Vol. 31, No. 10.

Williams, C. F.; Reed, M. J.; and Mariner, R. H., 2008, *A Review of Methods Applied by the U.S. Geological Survey in the Assessment of Identified Geothermal Resources*: U.S. Geological Survey Open-File Report 2008-1296, 27 p.